Coupling Investigation between RF Coil Array Elements backed by Surface Impedance Characterized Shields for 7 Tesla MRI

Zhichao Chen[1, 2], Klaus Solbach[2], Daniel Erni[1], and Andreas Rennings[1]

[1]General and Theoretical Electrical Engineering (ATE), Faculty of Engineering, University of Duisburg-Essen and CENIDE – Center for Nanointegration Duisburg Essen, D-47048 Duisburg, Germany

[2]High Frequency Engineering (HFT), Faculty of Engineering, University of Duisburg-Essen, D-47048 Duisburg, Germany

***Abstract*—In this paper we present a coupling investigation between RF coil array elements which are backed by surface impedance characterized RF shields for 7 Tesla magnetic resonance imaging (MRI). Two simulation models for the RF coil elements are considered here: an ideal impressed current model for an initial 2-D investigation, and a symmetrically fed dipole with meander terminals for the 3-D investigation. The RF shield, which is placed behind the coil element, is characterized by a surface impedance boundary condition (SIBC), where different surface impedances are defined. An optimal surface impedance of the RF shield can be found to achieve minimum coupling between neighboring coil elements. Different spatial arrangements (e.g. the shape of the phantom, the edge-to-edge separation between coupled coil elements, the separation from coil element to RF shield) are considered. In general, a large surface impedance provides a higher coupling level in comparison to a small surface impedance. As the separation distance from the coil element to the RF shield increases, a reduced surface impedance selectivity of the coupling behavior is observed. The proposed fundamental investigation reveals a new approach to modify the coupling characteristics of the dipole coil elements for MRI.**

***Index Terms*—Coupling, surface impedance boundary condition (SIBC), multi-channel RF coils, 7-Tesla MRI.**

I. Introduction

Over the last decade ultra-high field (UHF) MR imaging ($B_0 \geq 7$ T) has attracted more and more attention due to its enhanced imaging sensitivity, increased spectral resolution, and improved scan efficiency (parallel imaging techniques) [1]–[3]. However, associated with the increased magnetic field B_0, which is proportional to the Larmor frequency, the conventional RF coils, such as surface coils or volume coils, challenge the limits of design and performance. Among the arising issues for UHF MRI, a spatially inhomogeneous B_1 field and increased peak *SAR* are most critical for whole-body imaging [4], [5]. As one solution, multi-channel RF coils consisting of several coil elements have been applied to improve the coil performance for UHF MRI [5]–[8]. The overall magnetic field distribution can be tailored by the feeding (phase and amplitude) of individual coil elements according to the specific application. Symmetrically fed dipole elements have been widely used to build such multi-channel RF coils [8]–[10]. For such a dipole element a metallic plate, commonly called RF shield, is placed behind the dipole to prevent the interaction with the bore components of the magnetic resonance scanner [11]. So far, the effect of such a RF shield on the coupling between coil elements has not been rigorously studied.

Here, we systematically investigate the coupling between dipole coil elements, which are backed by surface impedance characterized RF shields. Two simulation models for the dipole coil element are considered here: an ideal impressed current model for two-dimensional investigation, and a symmetrically fed dipole with meander terminals for three-dimensional investigation. The RF shield is characterized by a surface impedance boundary condition (SIBC), where different surface impedances can be defined. An optimal surface impedance for a minimum coupling between neighboring coil elements is found by sweeping the surface impedance from extremely small to large values. Additionally, various spatial arrangements (e.g. the shape of the phantom, the edge-to-edge separation between coupled coil elements, the separation from coil element to RF shield) are also considered.

II. Coupling Investigation based on 2-D Models

Due to the simplicity of a 2-D model, a broad investigation in terms of geometry parameters, coil arrangements, and surface impedances of RF shield can be performed in an efficient manner.

A. Surface Impedance Boundary Condition

Surface impedance boundary conditions (SIBCs) are widely used to model the interface between two media where the main interest is focused only on one of them, and hence significantly simplifies the simulation domain in electromagnetic problems. The tangential components of both the electric and magnetic fields are associated through the surface impedance Z_s [12]:

$$\boldsymbol{E}_\mathrm{t} = Z_\mathrm{s}\ (\hat{\boldsymbol{n}} \times \boldsymbol{H}_\mathrm{t}), \tag{1}$$

where the index t refers to the tangential components, and $\hat{\boldsymbol{n}}$ is the unit vector normal to the corresponding SIBC. The SIBC is characterized by its surface impedance Z_s, which is swept from an extremely small value to a very large one in our study.

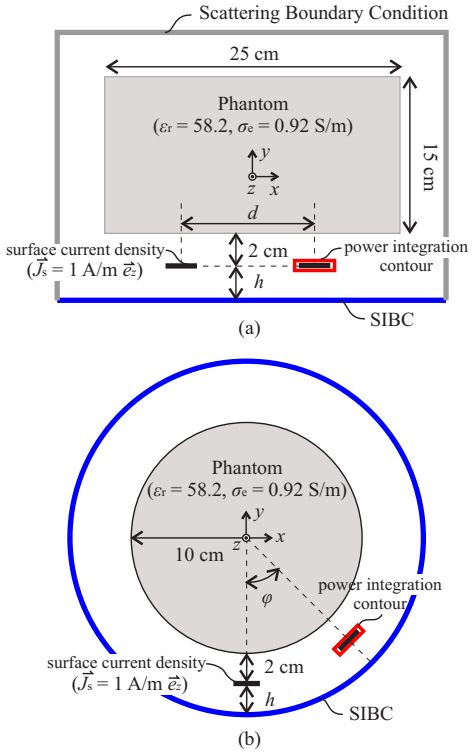

Fig. 1. Two-dimensional simulation models for the coupling investigation of dipole elements with surface impedance characterized RF shields: (a) two parallel aligned dipole elements loaded by a flat phantom, (b) two dipole elements azimuthally offset by angle φ around a cylindrical phantom.

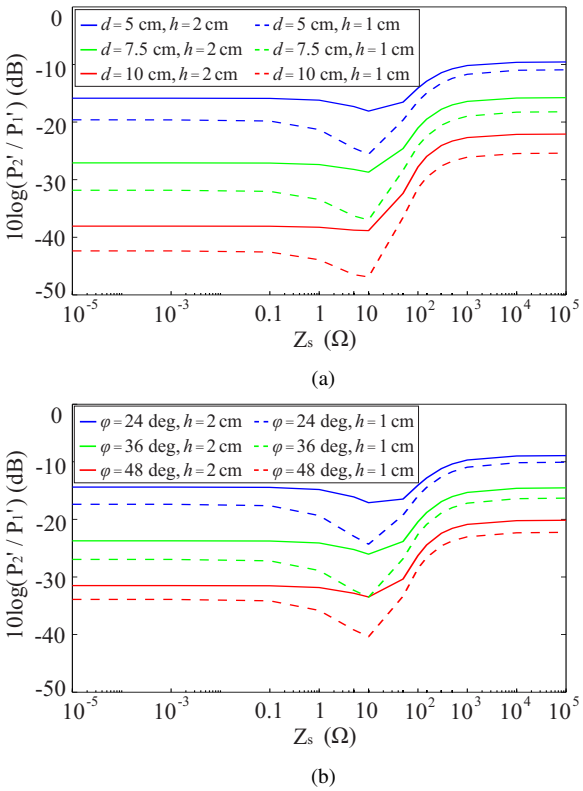

Fig. 2. Calculated power ratio P_2'/P_1' for the flat phantom arrangement (top) and the cylindrical phantom arrangement (bottom). P_1' and P_2' are the input power at the active element and the received power at the passive element, respectively. The effect of different separation distance from element to element (d, φ), and from element to RF shield (h) are investigated.

B. Simulation Setup

The two-dimensional simulation model in COMSOL Multiphysics for the coupling investigation of dipole elements is depicted in Fig. 1. Here we consider two different coil arrangements: two parallel aligned dipole elements loaded with a flat homogeneous phantom, and two dipole elements offset by an azimuthal angle around a cylindrical phantom. The same phantom parameters (ϵ_r = 58.2, σ_e = 0.92 S/m, ρ = 1000 kg/m^3) are utilized for the two aforementioned arrangements to emulate the human body for 7 T MRI, yielding an MR frequency of 300 MHz.

For the flat phantom arrangement, the coordinate system is placed in such a way that the x and y axis coincide with the horizontal and vertical direction, respectively, and the z axis points outward the figure. The SIBC terminating the simulation domain in negative y direction is located below the dipole element with a separation of h. The remaining boundaries of the simulation domain are assigned to a scattering boundary condition, which provides a sufficiently low reflection. Here, a 1.5 cm wide stripline shaped current sheet with an impressed surface current density J_s of 1 A/m in z-direction is used as the excitation of the electromagnetic field. The input power per unit length of this active element is calculated by

$$P_1' = -\frac{1}{2}\Re\{\int_C \boldsymbol{E}\cdot\boldsymbol{J}_\mathrm{s}\ \mathrm{d}c\}, \tag{2}$$

where $\boldsymbol{J}_\mathrm{s}$ and $\boldsymbol{E}$ are the impressed electric surface current density and the resulting electric field on the stripline (cf. Fig. 1), respectively. A passive element is aligned parallel to the active element with a center-to-center separation of d. The received power per unit length by this passive element can be computed by integrating the time averaged energy flux density through the integration contour (cf. Fig. 1), which encloses the passive element with a surface impedance of 50 Ω[1]:

$$P_2' = \frac{1}{2}\Re\{\int_S (\boldsymbol{E}\times\boldsymbol{H}^*)\cdot\mathrm{d}\boldsymbol{s}\}. \tag{3}$$

The coupling between the active and passive elements then can be evaluated by the ratio of P_2' and P_1'.

For the cylindrical phantom arrangement, the passive element is rotated by an azimuthal angle φ with respect to the phantom center. The angle φ (24°, 36°, 48°) is chosen in such a way that the azimuthal arc between the elements has the same length as the horizontal separation d (5 cm, 7.5 cm, 10 cm) for the flat phantom arrangement. The outer boundary of the simulation domain is assigned to SIBC, which models the RF shield. The power calculation for the active and passive elements remains unchanged in comparison to the case for a flat phantom.

[1]The surface impedance of the passive element is set to 50 Ω in order to model the 50 Ω port impedance in reality.

C. Simulation Results

The power ratio P_2'/P_1' for the two coil arrangements (cf. Fig. 1) is plotted versus surface impedance of the RF shield in Fig. 2. The effect of different separation distance from element to element, and from element to RF shield are investigated. In general, a large surface impedance provides a higher coupling level than a small surface impedance. Obviously, the coupling is stronger for a smaller separation between adjacent elements (d, φ). As the separation distance from the coil element to the RF shield (h) increases, a slightly reduced surface impedance selectivity of the coupling behavior is observed, indicated by a flatter curve for the power ratio. With the coil arrangement in Fig. 1, the minimum coupling between dipole elements appears for a surface impedance of 10 Ω. For extremely small and large surface impedances, the power ratio versus surface impedance is quite constant, indicated by a nearly flat curve. The power ratio is more sensitive to the surface impedance in the range $0.1\ \Omega \leq Z_s \leq 10^3\ \Omega$. Basically, the optimal surface impedance behaves in a similar manner for different coil arrangements, except that for a larger element-to-element separation (d, φ), the coupling for the cylindrical phantom arrangement is stronger than the one for the flat phantom arrangement. This phenomenon can be explained by the compressed electromagnetic field of the dipole elements due to the azimuthal offset.

III. Coupling Investigation Based on 3-D Models

In this the coupling characteristics between symmetrically fed dipole coil elements with surface impedance characterized RF shields is investigated based on a 3-D model.

A. Simulation Setup

The three-dimensional simulation model for the coupling investigation between dipole elements is depicted in Fig. 3, where a symmetrically fed dipole coil element with meander terminals is utilized. The total length of the coil element is 25 cm. The geometry of the meander remains unchanged in comparison to the structure in [10]. In order to fine-tune the current distribution on the strip line, high-dielectric substrates have been placed around the meander sections to increase their electrical length [13]. Similar to the two-dimensional investigation, a flat and a cylindrical phantom arrangement are considered. Phantom parameters are kept unchanged compared to Section II. The separation between neighboring elements for the flat phantom arrangement is set to d = 10 cm. For the cylindrical phantom arrangement the elements are offset by 48 deg in azimuthal direction, so that the azimuthal arc between the elements has the same length as the horizontal separation for the flat phantom arrangement. The separation between the element and the RF shield is fixed to 1 cm for the three-dimensional investigations.

B. Simulation Results

The simulated transmission coefficient $|S_{21}|$ of the coil arrangement (cf. Fig. 3) for different surface impedance of the RF shield are plotted in Fig. 4. For each surface impedance

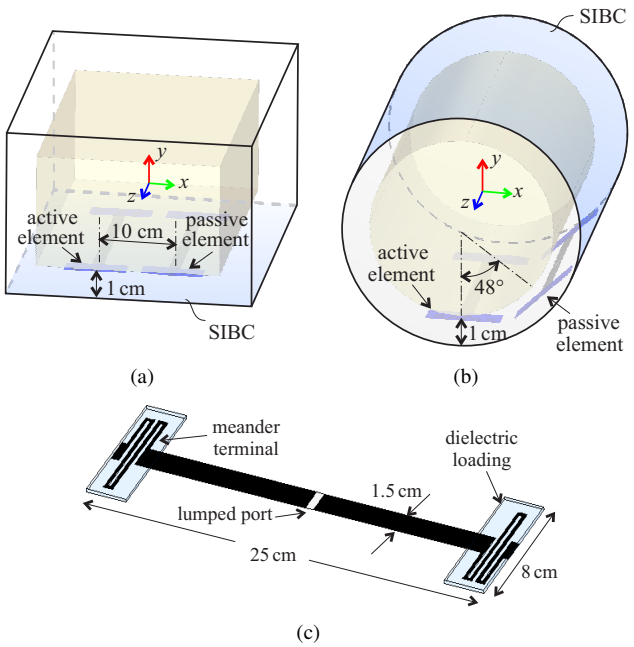

Fig. 3. Three-dimensional simulation models for the coupling investigation of dipole elements with surface impedance characterized RF shields. (a) Two parallel aligned dipole elements below a flat phantom. (b) Two azimuthally offset dipole elements around a cylindrical phantom. (c) Symmetrically fed dipole element with meander terminals, which are covered by high-dielectric material (ϵ_r = 10).

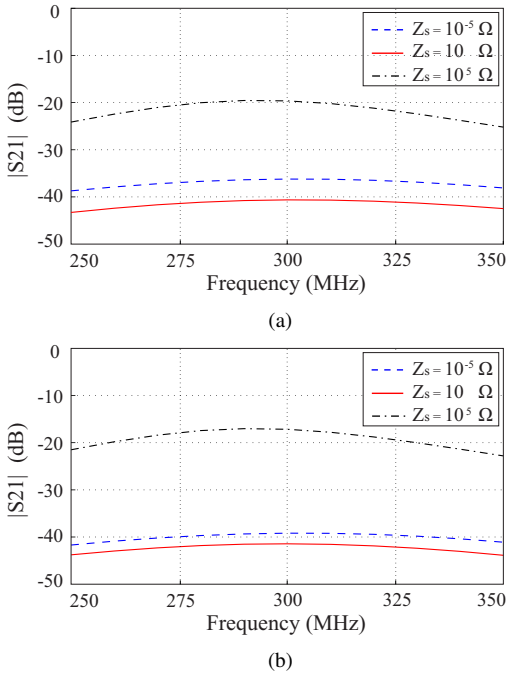

Fig. 4. Simulated transmission coefficient $|S_{21}|$ for (a) two parallel aligned dipole elements below a flat phantom, and (b) two azimuthally offset dipole elements around a cylindrical phantom.

a sufficient matching ($|S_{11}| \leq$ -25 dB) is achieved. The RF shield with large surface impedance (Z_S = 10^5 Ω) provides the highest coupling for the three compared cases. The coil elements with optimal surface impedance (Z_S = 10 Ω) from the

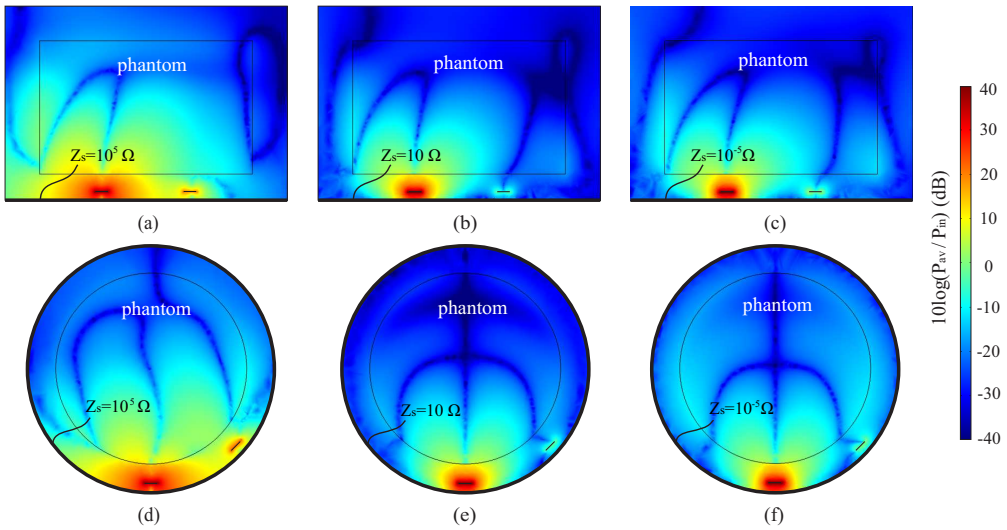

Fig. 5. Time-averaged energy flux density P_{av} in the transverse cut of the simulation domain for (a-c) two parallel aligned dipole elements loaded by a flat phantom (cf. Fig.3(a)), and (d-f) two azimuthally offset dipole elements loaded by a cylindrical phantom (cf. Fig.3(b)). The surface impedance of the RF shield for (a, d), (b, e) and (c, f) is assigned to 10^5 Ω, 10 Ω and 10^{-5} Ω, respectively. Z_{S} = 10 Ω refers to the case with the optimal decoupling.

two-dimensional investigation (cf. Fig. 2) reveal a minimum coupling at 300 MHz. The surface impedance $Z_{\text{S}} = 10^{-5}$ Ω behaves in a quite similar manner as the optimal case, but with a slightly higher coupling level. The minor difference between $Z_{\text{S}} = 10$ Ω and $Z_{\text{S}} = 10^{-5}$ Ω is in agreement with the flat curve for low surface impedance values in Fig. 2.

In order to understand the obtained coupling characteristics of the coil elements for different surface impedances, the time-averaged energy flux density P_{av} (i.e. Poyinting vector) in transverse cut ($z = 0$) of the simulation domain (cf. Fig. 5) was investigated. For a large surface impedance the energy flux density is focused in the vicinity of the coil element (outside the phantom) and extends to the neighboring element, resulting in a high coupling level. For a small surface impedance the coupling is mainly supported by the power flow inside the phantom. The different energy flux densities near the RF shield are due to the fact that the tangential electric field and normal magnetic field are supported by the boundary with large surface impedance, which is similar to a perfect magnetic conductor; whereas they are suppressed by the boundary with small surface impedance, which is similar to a perfect electric conductor. The minimum coupling is achieved with the optimal surface impedance, where the energy flux density in- and outside the phantom are moderately balanced.

IV. Conclusion

In this study we presented a coupling investigation of dipole elements with surface impedance characterized RF shield. Two simulation models for the dipole coil element have been considered here: an ideal impressed current model for 2-D analysis, and a symmetrically fed dipole with meander terminals for the 3-D case. Depending on the spatial arrangement (e.g. the shape of the phantom, the edge-to-edge separation between coupled coil elements, the separation from coil element to RF shield), an optimal surface impedance of the RF shield could be found for a minimum coupling between neighboring coil elements. The optimal surface impedance can be realized by a frequency selective surface (FSS) [14], which is currently under investigation. Our investigation reveals a new approach to modify the coupling characteristics of the dipole coil elements for 7 T MRI. The dipole elements utilized here are designed for 7 T MRI, however, the proposed approach is very general and can be applied to other MRI settings with different magnetic field strengths as well.

References

[1] M. E. Ladd, "High-Field-Strength Magnetic Resonance: Potential and Limits," *Top Magn Reson Imaging*, vol. 18, pp. 139–152, 2007.
[2] E. Moser *et al.*, "7-T MR from research to clinical applications?" *NMR Biomed.*, vol. 25, pp. 695–716, 2012.
[3] P.-M. Robitaille and L. J. Berliner, *Ultra High Field Magnetic Resonance Imaging*, ser. Biological Magnetic Resonance. Springer, 2006, vol. 26.
[4] J. T. Vaughan *et al.*, "7T vs. 4T: RF power, homogeneity, and signal-to-noise comparison in head images," *Magn. Reson. Med.*, vol. 46, no. 1, pp. 24–30, 2001.
[5] P.-F. Van de Moortele *et al.*, "B_1 destructive to interferences and spatial phase patterns at 7 T with head transceiver array coil," *Magn. Reson. Med.*, vol. 54, pp. 1503–1518, 2005.
[6] J. T. Vaughan *et al.*, "Efficient High-Frequency Body Coil for High-Field MRI," *Magn. Reson. Med.*, vol. 52, pp. 851–859, 2004.
[7] G. Adriany *et al.*, "Transmit and receive transmission line arrays for 7 Tesla parallel imaging," *Magn. Reson. Med.*, vol. 53, pp. 434–445, 2005.
[8] A. J. E. Raaijmakers *et al.*, "Design of a Radiative Surface Coil Array Element at 7 T: The Single-Side Adapted Dipole Antenna," *Magn. Reson. Med.*, vol. 66, pp. 1488–1497, 2011.
[9] D. O. Brunner *et al.*, "A symmetrically fed microstrip coil array for 7T," in *15th Proc. Intl. Soc. MRM*, 2007, p. 448.
[10] S. Orzada *et al.*, "A novel 7 T microstrip element using meanders to enhance decoupling," in *16th Proc. Intl. Soc. MRM*, 2008, p. 2979.
[11] J. T. Vaughan and J. R. Griffiths, Eds., *RF Coils for MRI*. Wiley, August 2012.
[12] S. Tretyakov, *Analytical Modeling in Applied Electromagnetics*. Artech House, 2003.
[13] Z. Chen *et al.*, "Dipole RF Element for 7 Tesla magnetic resonance imaging with minimized SAR," in *7th Eur. Antennas and Propag. Conf.*, Göteborg, Sweden, April 8-12, 2013, pp. 1716–1719.
[14] N. Engheta and R. W. Ziolkowski, Eds., *Metamaterials: Physics and Engineering Explorations* . Wiley-IEEE Press, August 2006.